Angular dependence of the disorder crossover in the vortex lattice of $Bi_{2.15}Sr_{1.85}CaCu_2O_{8+\delta}$ by muon spin rotation and torque magnetometry

C. M. Aegerter, J. Hofer, I. M. Savić, and H. Keller
Physik-Institut der Universität Zürich, CH-8057 Zürich, Switzerland

S. L. Lee and C. Ager
School of Physics and Astronomy, University of St. Andrews, St. Andrews, Fife KY169SS, United Kingdom

S. H. Lloyd and E. M. Forgan
School of Physics and Space Research, University of Birmingham, Birmingham B15 2TT, United Kingdom
(Received 11 July 1997)

Using the techniques of muon spin rotation and torque magnetometry, we investigate the crossover field B_{cr} in $Bi_{2.15}Sr_{1.85}Ca_1Cu_2O_{8+\delta}$ at which the vortex lattice becomes disordered along the field direction. It is found that B_{cr} scales as the projection of the applied field along the perpendicular to the superconducting planes. This has the implication that a field large enough to give a disordered lattice when applied perpendicular to the planes, can give a well-ordered vortex-line lattice for angles of the field to the c axis greater than a critical value. [S0163-1829(98)09401-6]

I. INTRODUCTION

Cuprate superconductors exhibit a strongly anisotropic superconducting behavior. This is due largely to their layered structure, which favors supercurrents flowing in the CuO_2 planes. The high-temperature superconductor $Bi_{2.15}Sr_{1.85}Ca_1Cu_2O_{8+\delta}$ (BSCCO) is extremely anisotropic, quantified by the anisotropy parameter $\gamma=\lambda_c/\lambda_{ab}\sim 150$, where λ_c, λ_{ab} are the penetration depths for currents flowing perpendicular and parallel to the superconducting planes. This extreme anisotropy, together with the high operating temperatures of these high-T_c superconductors, leads to very unusual behavior of flux vortices, such as vortex lattice melting.[1,2]

In highly anisotropic systems such as these, the flux lines are best viewed as a weakly coupled stack of quasi-two-dimensional (2D) ''pancake'' vortices, each confined to a superconducting plane.[3–5] At low fields and temperatures these stacks may resemble conventional vortex lines, but with increasing fields the response of the system to elastic deformations will change. In this continuum limit the elastic constants used to describe the system are highly dispersive. Above a certain field the energetic cost of interlayer deformations of the lattice, on small scales, becomes less than the cost of intralayer deformations within the superconducting planes. In the extreme limit, where this length scale equals the interlayer separation, positional fluctuations can then occur between the pancake vortices in adjacent layers belonging to a vortex line. A characteristic field, above which disorder along the field direction occurs, has been identified in BSCCO using muon spin rotation (μSR) and small-angle neutron scattering (SANS).[4–6] This could be identified with the onset of ''vortex entanglement,'' as predicted theoretically.[7] Previous μSR studies have suggested that the characteristic wavelength in the c direction of transverse fluctuations of vortices may be comparable to the interlayer separation s, so one might view this as a ''dimensional crossover.'' We shall simply refer to this as the crossover field B_{cr}. This crossover is closely related to the so-called ''fishtail'' or ''second-peak'' effect in magnetization hysteresis loops. Many authors have ascribed the fishtail solely to pinning effects,[8,9] although it has been shown that the value of the magnetic field at which a *microscopic* change in the vortex structure, as observed at low temperatures with μSR, coincides exactly with the appearance of the fishtail.[10,11] This microscopic change of the flux structure above B_{cr} is probably accentuated, since short segments of the softening vortex lines can adjust more easily to the random pinning potential. A static disordering of the vortex lines along their length thus occurs. We note that many observable features of this crossover occur because of the influence of the point pinning sites on the vortex lines. This is true for magnetization peak effects, μSR, and small-angle neutron-scattering (SANS) measurements.[4,5,10,11,6] For instance, in macroscopic magnetization measurements the fishtail is due to a sudden increase of the magnetization, which arises from a change in response of the vortices to pinning. We note, however, that these changes most likely reflect the underlying changes in the effective rigidity of the vortex system.

For a strongly Josephson coupled system B_{cr} occurs when the vortex separation a equals the width of the Josephson vortex core γs, which gives $B_{cr}=B_J\sim\phi_o/(\gamma s)^2$, where ϕ_o is the flux quantum. Recent work suggests that in systems of very large anisotropy, such as BSCCO, this expression may need to be modified in in the limit $\lambda_{ab}<\gamma s$.[5,12,13] This is because at the field where a first exceeds γs, the vortices are still rather dilute, so are well correlated along the c direction and little distorted by intraplane interactions. The crossover is therefore pushed to a higher field $B_{cr}=B_\lambda\sim\phi_o/\lambda_{ab}^2$, which is the field where the vortices start to overlap strongly.

In this paper we present studies of the angular dependence of the crossover field in BSCCO. We combine μSR mea-

 © 1998 The American Physical Society

surements with torque magnetometry, and show that the signatures revealing the crossover field by both techniques are well correlated. The simple scaling relation which is revealed leads to a simple interpretation of the angular dependence.

II. EXPERIMENT

The BSCCO samples used for the μSR experiments consisted of a mosaic of overdoped single crystals ($T_c = 85$ K), grown using a floating-zone technique described elsewhere.[14] The platelike samples, which have their c axes perpendicular to their largest face, were mounted with these axes perpendicular to the sample holder. The μSR measurements were carried out on beamline πM3 at the Paul Scherrer Institute, Villigen, Switzerland, and the torque measurements on a homebuilt torque magnetometer at University of Zurich using one single crystal taken from the μSR mosaic.

The μSR experiment uses surface muons of momentum 29 MeV/c, which are spin polarized with their spins perpendicular to their momentum direction. The sample is subjected to a magnetic field which is directed parallel to the incident muon momentum. The muons decay after an average lifetime of 2.2 μs, emitting positrons preferentially along their spin direction.[15] The muons arrive randomly at the sample where they rapidly thermalize and then precess in the local magnetic field. Before the muons hit the sample they pass through a muon detector which starts a clock. Positron detectors placed around the sample measure the number of positrons emitted along a given direction as a function of this clock time. Logic gating of the pulses ensures that the only events accepted are those in which only one muon is present in the sample at any given time. By time-binning large numbers of the detected positron events, a time spectrum is built up which reflects the muon precession within the sample. Inside the mixed state of the superconductor the presence of the vortex lattice gives rise to a spatial modulation of the local flux density $B(r)$. Since the muons are implanted randomly with respect to the vortex lattice, the range of precession frequencies reflects this internal flux distribution. By Fourier transforming the muon time spectra one obtains the μSR line shape, or frequency distribution. This is an excellent measure of the probability distribution of internal field values of the superconductor, $p(B)$. The μSR line shape is thus intimately related to the spatial distribution $B(r)$, so can be used to deduce important structural information on the vortex lattice.[4,16,5,12]

For our analysis we require the μSR line shape, which is a Fourier transform of the positron decay spectrum, in order to obtain $p(B)$. While conventional Fourier methods may be used, we prefer to utilize a maximum entropy method which suppresses noise due to Poisson counting statistics which would always be present in a conventional Fourier analysis technique.[17] This is useful if one wants to perform systematic analysis on moments of $p(B)$, which can be extremely sensitive to the presence of random noise. Without any constraints, a uniformly flat distribution $p(B_i) = \text{const}$ will maximize the entropy

$$S = \sum p(B_i) \ln(p(B_i)/d_i), \tag{1}$$

where d_i represent default values, which in the analysis were assumed to constitute a flat distribution. In order to obtain the desired field distribution, maximizing the entropy has to be constrained by the data. This is done by introducing the usual quantity $\chi^2 = \Sigma (n_i - y_i)^2/\sigma_i^2$, where n_i are the time domain data, after correction for the exponential decay of the muon, σ_i^2 are the associated experimental errors, and y_i constitute the Fourier transform of the calculated field distribution. We then obtain the desired field distribution by minimizing the quantity

$$L = S - \lambda \chi^2, \tag{2}$$

where λ is a Lagrange multiplier. In this way our maximum entropy algorithm results in the most uniform distribution which is consistent with the data. Some degree of freedom in weighting the χ^2 argument with respect to the entropy argument can now be gained by artificially increasing χ^2 through scaling the errors σ_i by a small fraction. One can thus optimize the agreement between the data and the calculated field distribution by increasing the weight of χ^2. The criteria we use is to choose that scaling factor which is closest to unity, but which will not increase the noise in the distribution such that the moments can no longer be calculated with confidence. That is, we aim to produce a spectrum which is flat outside of the region of interest. Once this has been achieved, the scaling factor must remain constant for the remainder of a systematic analysis. In the following analysis we used a scaling factor of 1.03. While the choice of this parameter can lead to systematic variations in the spectra, these should be compared with variations which may be introduced in conventional Fourier techniques, such as apodization of the time window. In our method the data itself never undergoes Fourier transformation, so we avoid problems associated with transforming experimental noise. The moments of the distribution may thus be easily evaluated. To avoid artefacts due to systematic variations, for a given analysis we ensure that all data sets have similar counting times and hence similar errors. In summary, the maximum entropy technique should be used with care, but correctly used it provides a very powerful method for examining subtle details of the μSR spectra, not easily possible by other techniques.

For the μSR measurements the sample was mounted on an Fe_2O_3 backing plate, as described in Refs. 4,18. The purpose of this is to reduce the contributions to the μSR spectra from those muons which to do not stop in the sample, but which land outside of the sample or pass through if the samples are thin. Any muons landing in the antiferromagnet Fe_2O_3 rapidly depolarize, outside of the observable time window. The recorded spectra thus arise only from muons inside the superconductor. By rotating the sample holder, measurements could be performed for many angles of the applied field to the crystallographic c direction. This allowed the angular dependence of the vortex behavior to be determined.

The magnetization data was gathered using torque magnetometry. The BSCCO crystals were measured using a cantilever sensor constructed from phosphor bronze (see Ref. 19). A magnetic moment $\vec{m}$ in a field $\vec{B}$ experiences a torque $\vec{\tau} = \vec{m} \times \vec{B}$. In our torque magnetometer this torque is mea-

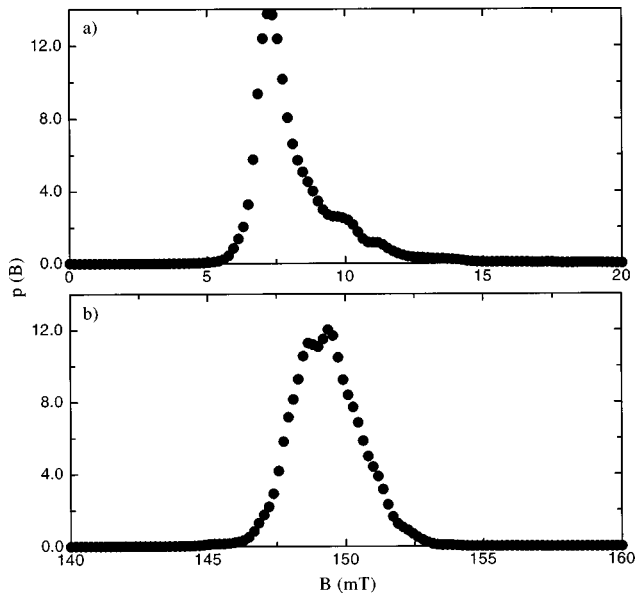

FIG. 1. Probability distributions of internal flux density $P(B)$ in BSCCO at 5 K, as determined by μSR, for fields applied parallel to the c direction. (a) The $p(B)$ for an applied field of 10 mT, showing a typical line shape for a vortex line lattice. The tail towards high fields arises from fields close to the vortex cores (see text). (b) A typical line shape for fields above the disorder crossover B_{cr}. The truncation of the high-field tail arises from a wandering of the vortex line along the field direction (see text).

sured by the deflection of a capacitive spring.[19] Except for angles of the field very close to the ab planes, $\vec{m}$ is always directed along the c axis, so $\vec{m}$ can readily be calculated from the measured torque.

III. RESULTS AND DISCUSSION

The field distribution in the mixed state of type-II superconductors has been calculated, e.g., by Sidorenko *et al.*[20] For a lattice of straight vortex lines, the field distribution shows a distinct weighting towards fields higher than the average. This is due to the very high fields present in the vortex cores. This is illustrated in Fig. 1(a), which shows a measured line shape for BSCCO with a field of 10 mT directed along the c direction. The expected distribution above the crossover field is quite different, as disorder along the flux lines effectively smears the core fields, thus leading to a truncation of the high-field tail in the field distribution, as illustrated in Fig. 1(b). The crossover field can therefore be observed in both the width of the distribution and its shape, as it should become much more symmetric with the truncation of the high-field tail.[5,4] We quantify the skewness of the field distribution by a quantity derived from the ratio of the third and second moments

$$\alpha = \frac{\sqrt[3]{\langle \Delta B^3 \rangle}}{\sqrt{\langle \Delta B^2 \rangle}}. \tag{3}$$

A positive value of α indicates a weighting of the distribution towards high fields. A symmetric distribution will be quantified by $\alpha = 0$. For an ideal lattice of vortex lines, α is expected from numerical simulations to be ~ 1.2 for our experimental setup. In Fig. 2 we show the field dependence of α for different angles. The crossover field is manifested by a drop in α from its initial value of ~ 1.2 to ~ 0.6, indicating a much more symmetric line shape. It can be seen in the figure, that the crossover takes place at higher fields and is also smeared over a wider range of fields if the applied field is at a large angle to the c axis. We determine the crossover field from the point where α becomes approximately independent of the applied field. This occurs at a lower value of $\alpha \sim 0.6$, where we have applied the same criterion previously used to determine the crossover field parallel to the c axis.[4,5]

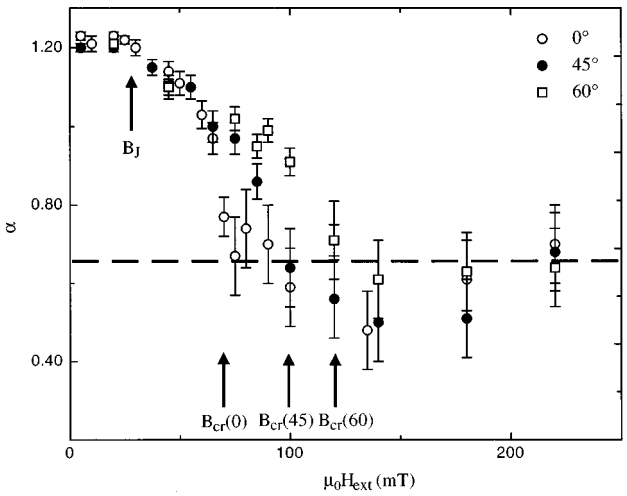

FIG. 2. The field dependence of the skewness parameter $\alpha = \langle \Delta B^3 \rangle^{1/3} / \langle \Delta B^2 \rangle^{1/2}$, which describes the μSR line shape. The data is measured after cooling to 5 K, in a field applied at various angles ϑ to the c direction. The disorder crossover field is indicated by an arrow, where α has dropped from its initial value of 1.2 to ~ 0.6 (see text). The crossover field clearly depends on the angle of the applied field to the c axis.

The results of $B_{cr}(\vartheta)$ are summarized in Fig. 3. We have also determined $M(H)$ loops at various different angles of the field with respect to the c axis. As is well known in the literature, these $M(H)$ loops exhibit a characteristic structure showing two peaks, as shown in Fig. 4(a). In Fig. 4(b) it can be seen that the microscopic change in the field distribution observed by μSR takes place at the deviation of the magnetization from the usual type-II behavior, that is, around the second peak in $M(H)$.[10,11] To agree with the observed crossover in the μSR data, values of the crossover field in Fig. 3 from torque magnetometry are determined from the point of maximum slope of the magnetization at the second peak, which may be seen from the differential of the magnetization also plotted in Fig. 4(b). We see from Fig. 3 that the angular dependence of the crossover field as determined by the two methods of μSR and torque magnetometry both agree, and are well described by the relation

$$B_{cr}(\vartheta) \approx B_{cr}(0)/\cos(\vartheta). \tag{4}$$

The crossover field thus effectively depends upon the projection of the applied field along the c direction. This appears to be in accord with the scaling approach of Blatter *et al.*,[21] for anisotropic superconductors in the presence of isotropic disorder. This would predict an angular scaling

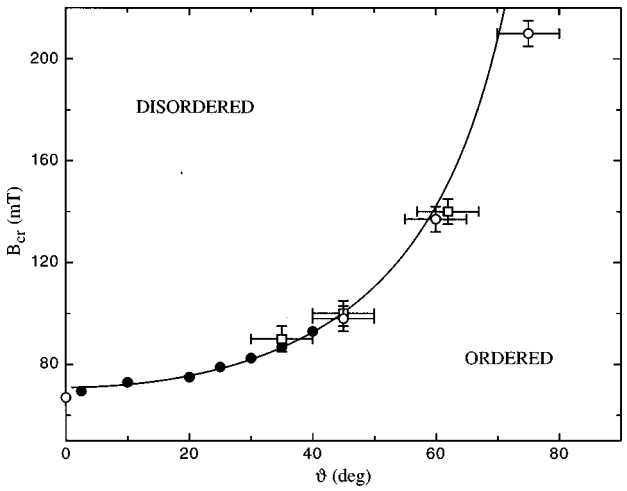

FIG. 3. The angular dependence of the crossover field of BSCCO, as determined from different methods. Open symbols are μSR measurements obtained from the field dependence of the skewness parameter α (circles) and from the angular dependence of the μSR linewidth (squares) (see text, Fig. 5). The error bars in the μSR measurements originate from an uncertainty in the alignment of the crystals of the mosaic used in the measurements. Filled circles are derived from torque measurements, where the crossover field is determined from the appearance of a second peak in $M(H)$ loops (cf. Fig. 4). The solid line corresponds to Eq. (4).

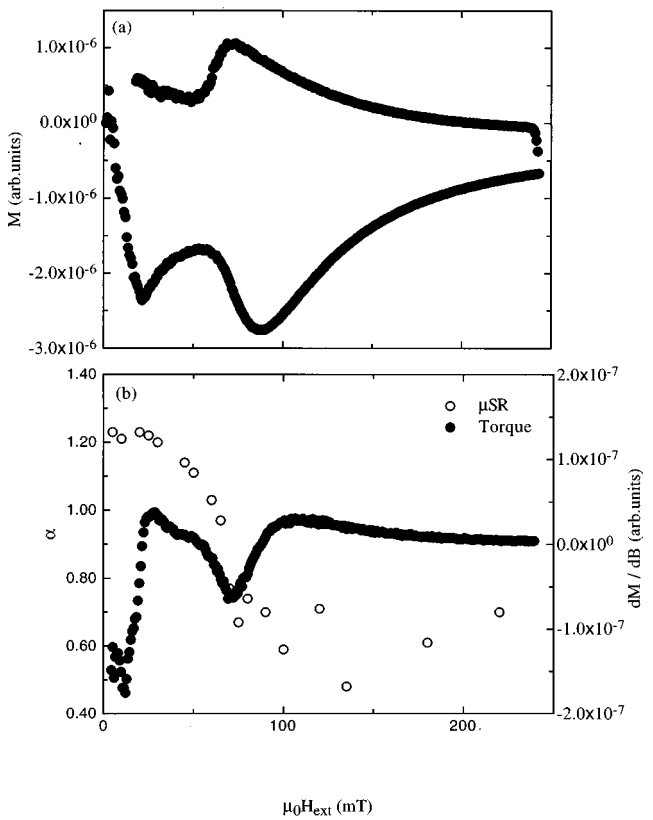

FIG. 4. (a) A typical $M(H)$ loop as obtained from torque magnetometry. The field is at an angle of 2.5° to the c axis. (b) The μSR line-shape parameter α as a function of field applied parallel to c, indicating the microscopic change in the field distribution at B_{cr}. The differential of the curve in (a) is also overlaid, from which it can be seen that the maximum slope in the magnetization coincides with the crossover field as defined in Fig. 2. We thus determine the crossover field from $M(H)$ loops from the point of maximum slope in M before the second peak (see text).

$$B_{cr}(\vartheta)=\frac{B_{cr}(0)}{(\cos^2\vartheta+1/\gamma^2\sin^2\vartheta)^{1/2}}, \tag{5}$$

which for large γ reduces to Eq. (4). This agreement is, however, rather suprising, given that the crossover occurs at low field, outside the region of validity of the Blatter scaling relation.

With reference to Fig. 2, we note that the apparent rolloff of α at around 25 mT is remarkably angle independent. In Ref. 12 it was shown that around 20 mT there exists a change in the temperature dependence of the vortex lattice melting line, as measured by μSR. This was found to be highly consistent with the predictions of Ref. 22 , which considers the role of electromagnetic coupling in determining the phase diagram of BSCCO. This position of this feature in the melting line has been interpreted as $B_J \sim \Phi_0/(\gamma s)^2$, the field where the cores of the Josephson vortices start to overlap.[12,22] In Ref. 5 the onset of the angle-independent rolloff in α as a function of field was also associated with B_J. This may be understood as the field above which Josephson currents become ineffective at screening the phase fluctuations arising from pancake vortex displacements in neighboring layers. Electromagnetic coupling then begins to dominate the single vortex line tension, which could lead to a ''softening'' of the vortex lines at shorter length scales.

Another manifestation of the angular dependence of the crossover field arises from the angular dependence of the second moment of the μSR line shape. For a lattice of straight vortex lines, the second moment is expected to scale with the angle of the field with respect to the c axis as[18,20,23]

$$\langle \Delta B^2\rangle^{1/2}(\vartheta)=\langle \Delta B^2\rangle^{1/2}(0)(\cos^2\vartheta+1/\gamma^2\sin^2\vartheta)^{1/2}, \tag{6}$$

which for compounds as anisotropic as BSCCO reduces to $\langle \Delta B^2\rangle^{1/2}(\vartheta)=\langle \Delta B^2\rangle^{1/2}(0)\cos(\vartheta)$. This behavior is due to the direct connection of the μSR linewidth with the penetration depth of the samples and has been observed in the moderately anisotropic $YBa_2Cu_3O_{6+x}$.[24] For fields below the crossover field we observe a similar angular dependence in BSCCO as is evident from Fig. 5. For fields well above the crossover field, however, a linewidth only weakly dependent on the angle of the applied field is observed (cf. Fig. 5, Ref. 18). This can be understood in terms of the pinning-induced disorder of the vortex lattice above B_{cr}, as described above. Random lateral displacements of vortices in neighboring layers, due to pinning will induce phase fluctuations of the order parameter. This will also lead to a random array of Josephson vortices, generating fields parallel to the planes. There is thus a large variation in the local field distribution arising from all components of the internal field. Hence, disorder continues to dominate the field distribution, even when the field is tilted away from the c axis. As a result, the second moment remains largely independent of angle, even for quite

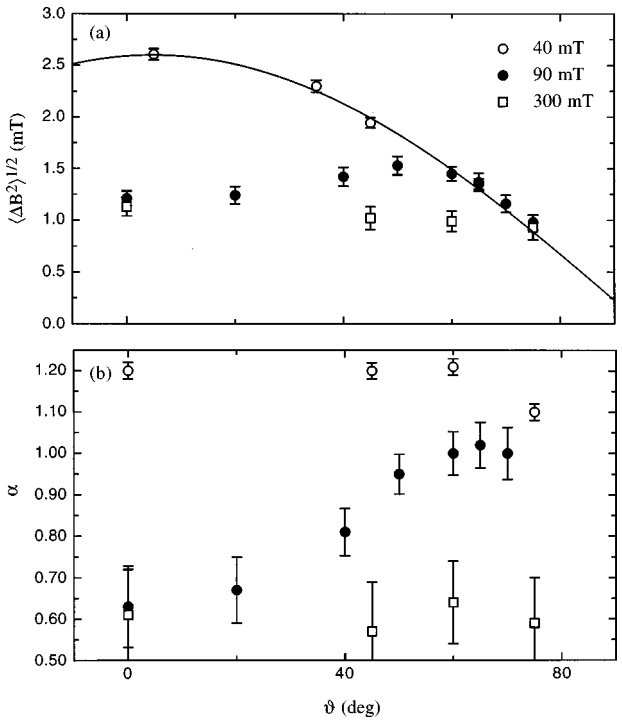

FIG. 5. (a) The second moment of the μSR line shape as a function of the angle of the field with respect to the c axis. For fields lower than the crossover field (e.g., 40 mT) the angular dependence is as expected for a lattice of straight vortex lines [Eq. (4)], whereas for very high applied fields (e.g., 300 mT) it is only weakly dependent on the angle Ref. 18. This is due to the disordered nature of vortex arrangement above the crossover field (see text). For intermediate fields, one observes a crossover between these two limits, as can be seen in the 90 mT data. From the angle at which the crossover happens ($\vartheta \approx 40°$ for 90 mT), we have another determination of the angular dependence of the crossover field. (b) The line-shape asymmetry parameter α [see Eq. (3)] as a function of angle as above. At low fields (e.g., 40 mT) the value of α is as expected for an ideal vortex line lattice (see text) for all angles. At high fields (e.g., 300 mT) α is again independent of the angle, but has a value reflecting the disorder present above the crossover. For intermediate fields (e.g., 90 mT) the rise in α above some critical angle reflects the increasing order in the vortex lattice as B effectively falls below the crossover field (see text). This change in α is a measure of the change in the line-shapes seen in Fig. 6. The data are all field-cooled measurements at 5 K.

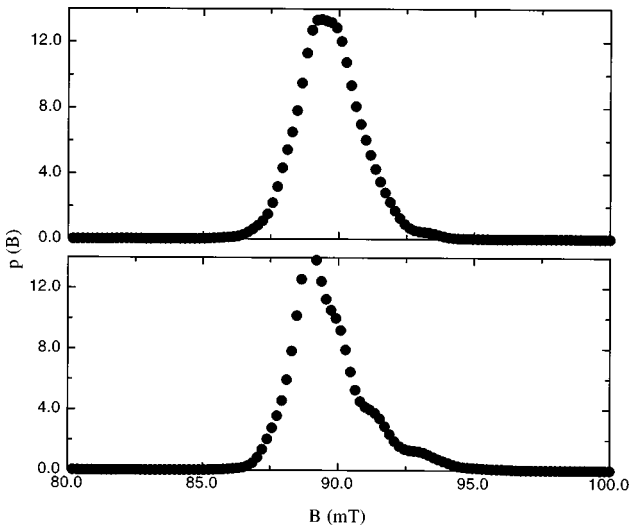

FIG. 6. Examples of the μSR line shapes measured below and above the angle at which the c-axis component of the field falls below $B_{cr}(0)$. The data were measured after cooling in 90 mT applied at angles of $\sim 0°$ and $\sim 60°$, respectively. It can be seen from the line shape that at high angles, there is increased weighting towards high fields, indicating that the vortices are more ordered along the field direction. This is because at high angles the applied field is effectively below the crossover field (see text).

large values of ϑ. An interesting phenomenon occurs if the angle ϑ is such that the component of B along the c axis is smaller than the crossover field, $B\cos(\vartheta) < B_{cr}(0)$. In this case the pancake vortices appear to move towards being well aligned along the field direction, which is manifest in two ways. Firstly, the asymmetry parameter α rises towards its ideal lattice value, as can be seen by the clear change of line shape at 90 mT, above and below $\sim 40°$, in Figs. 5 and 6. Secondly, the angular variation of the second moment rejoins the angular dependence which would be expected for a well ordered lattice, as depicted in Fig. 5. We interpret this as follows. The scaling of Eq. (5) implies that as the angle increases above some critical angle ϑ_c, the applied field B will be less than the angular-dependent crossover field, that is $B < B_{cr}(\vartheta_c)$. For high angles the lattice thus becomes more ordered. Taking $B = 90$ mT yields $\vartheta_c \sim 41°$, consistent with the observed change of behavior at $\sim 40°$. Conversely, we can thus estimate the value of the crossover field at certain angles from such changes of behavior of the angular dependence of the μSR linewidth. Some estimates of the crossover using this method are also included in Fig. 3.

In conclusion, we have studied the disorder crossover field in BSCCO using the techniques of μSR and torque magnetometry. We find that the crossover field scales with the field component in the c direction. This result is obtained from both a microscopic change in the field distribution as shown by μSR, and from the deviation of $M(H)$ loops from the usual type-II behavior in the so-called fishtail. We have also studied the angular dependence of the width of the field distribution in μSR for different applied fields. We find the expected angular dependence for fields below the crossover, whereas it is only weakly dependent on the angle for very high fields. In an intermediate regime however, where the applied field is $B \gtrsim B_{cr}(0)$, we find a more complex behavior, observing a crossover of the lattice from disordered to quasiordered with increasing angle. From this we are also able to determine the angular dependence of the crossover field, which is in good agreement with that determined from the skewness of the field distribution.

ACKNOWLEDGMENTS

We would like to thank T. W. Li (University of Leiden) for the preparation of the crystals, and the staff on beamline πM3 at PSI, Zürich, for technical support. Financial support from the Swiss National Science Foundation and the EPSRC of the UK is gratefully acknowledged.

[1] G. Blatter *et al.*, Rev. Mod. Phys. **66**, 1125 (1995).
[2] M. P. A. Fisher, D. S. Fisher, and D. A. Huse, Phys. Rev. B **43**, 130 (1991).
[3] L. I. Glazman and A. E. Koshelev, Phys. Rev. B **43**, 2835 (1991).
[4] S. L. Lee *et al.*, Phys. Rev. Lett. **71**, 3862 (1993).
[5] C. M. Aegerter *et al.*, Phys. Rev. B **54**, R15 661 (1996).
[6] R. Cubitt *et al.*, Nature (London) **365**, 407 (1993).
[7] D. Ertas and D. R. Nelson, Physica C **272**, 79 (1996).
[8] V. N. Kopylov *et al.*, Physica C **170**, 291 (1990).
[9] N. Chikumoto *et al.*, Phys. Rev. Lett. **69**, 1260 (1992).
[10] G. Yang *et al.*, in *Proceedings of the 7th International Workshop on Critical Currents in Superconductors*, Alpad, Austria, 1994, edited by H. W. Weber (World Scientific, Singapore, 1994), p. 264.
[11] C. Bernhard *et al.*, Phys. Rev. B **52**, R7050 (1995).
[12] S. L. Lee *et al.*, Phys. Rev. B **55**, 5666 (1997).
[13] V. M. Vinokur (private communication).
[14] T. W. Li *et al.*, J. Cryst. Growth **135**, 481 (1994).
[15] B. Pümpin *et al.*, J. Less-Common Met. **164&165**, 994 (1990).
[16] S. L. Lee *et al.*, Phys. Rev. Lett. **75**, 922 (1995).
[17] B. D. Rainford and G. J. Daniell, Hyperfine Interact. **87**, 1129 (1994).
[18] R. Cubitt *et al.*, Physica C **213**, 126 (1993).
[19] D. Zech *et al.*, Phys. Rev. B **54**, 12 535 (1996).
[20] A. D. Sidorenko, V. P. Smilga, and V. I. Fesenko, Hyperfine Interact. **63**, 49 (1990); Physica C **166**, 167 (1990).
[21] G. Blatter *et al.*, Phys. Rev. Lett. **68**, 875 (1992).
[22] G. Blatter *et al.*, Phys. Rev. B **54**, 72 (1996).
[23] S. L. Thiemann *et al.*, Phys. Rev. B **39**, 11 406 (1989).
[24] E. M. Forgan *et al.*, Hyperfine Interact. **63**, 71 (1990).